J|A|C|S COMMUNICATIONS

Published on Web 04/29/2009

Microstructured Materials Based on Multicompartmental Fibers

Srijanani Bhaskar and Joerg Lahann*

Departments of Macromolecular Science and Engineering, Chemical Engineering, and Materials Science and Engineering, University of Michigan, Ann Arbor, Michigan 48109

Received January 23, 2009; E-mail: lahann@umich.edu

Ⓦ **This paper contains enhanced objects available on the Internet at http://pubs.acs.org/jacs.**

Electrospinning of natural and synthetic functional polymers is a common technique used to generate aligned fibers of varying diameters, and the potential use of these fibers in tissue engineering has been studied extensively.[1−3] However, the ability to control the fiber microarchitecture and thereby important biological functions, such as spatially controlled presentation of biomolecules,[4] is a key challenge in regard to successful tissue regeneration.[5−7] In this communication, we demonstrate a novel type of microstructured scaffold material comprising multicompartmental microfibers. These scaffolds are prepared by electrohydrodynamic cospinning of two or more poly(lactide-*co*-glycolide) (PLGA) polymers, which yields biodegradable microfibers with multiple, chemically distinct compartments. The novel cospinning process used to prepare these multicompartmental microfiber scaffolds was inspired by a recent synthesis of bi- and triphasic particles that exploited electrohydrodynamic cojetting of aqueous polymer solutions.[8−12] In multicompartmental microfibers, individual compartments can differ with respect to their chemical compositions, which are controlled by controlling the chemical composition of the initial jetting solutions. Thus, individual compartments may consist of a palette of different additives, such as functional polymers, dyes, or biomolecules (Figure 1a). Figure 1b,c shows scanning electron microscopy (SEM) and confocal laser scanning microscopy (CLSM) micrographs of a typical bicompartmental microfiber scaffold made by electrohydrodynamic cojetting. The SEM image corroborates the high degree of alignment and the narrow size distribution of the microfibers, while the internal architecture is characterized by distinct red and blue compartments, as confirmed by the CLSM image. Extremely sharp boundaries are observed at the interfaces between compartments, suggesting minimal mass transfer between the compartments.

Several cooperatively acting parameters, including high viscosity of the jetting solution, low flow rates, and high solvent volatility, contribute to the formation of a continuous jet, which appears to be only minimally affected by the temporal perturbations typically observed during electrospinning.[13] The jet stability is further exemplified by employing a ternary nozzle configuration. Figure 2 shows CLSM images of a group of microfibers, each of which comprises three individual compartments. In spite of the increase in complexity due to the transition from two to three outlet streams, the new fibers show the same high-precision alignment of the fibers and compartments as observed previously for bicompartmental microfiber scaffolds. In fact, extraordinarily stable jets were often sustained for several hours.

When microstructured fibers with more than two compartments are fabricated, the configuration of the individual compartments becomes another design parameter. For a fiber with three equally sized compartments observed in a three-dimensional space, there are in theory four optically distinguishable permutations. The corresponding "isomers" consist of fibers with three striped (s) compartments, i.e., red−blue−green {sRBG}, blue−red−green {sBRG}, and blue−green−red {sBGR} fibers.

In addition, one trigonal isomer exists, which we will label as a "pie-shaped" (p) fiber, {pRGB}. To demonstrate the versatility of the electrohydrodynamic cospinning approach, we set forth a series of experiments to prepare all four of the theoretically possible isomers for a tricompartmental fiber [details regarding the synthesis and CLSM imaging are provided in the Supporting Information (SI)]. We next

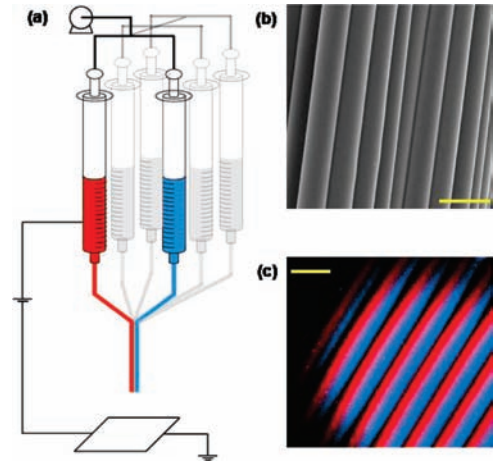

Figure 1. (a) Schematic representation of the cojetting process using a dual capillary assembly (red and blue). This approach can be extended to fabrication of multicompartmental microfibers by incorporating additional outlet streams (gray). (b) SEM image of a bicompartmental microfiber scaffold. (c) CLSM image of bicompartmental microfibers. Scale bars in (b) and (c) represent 20 μm.

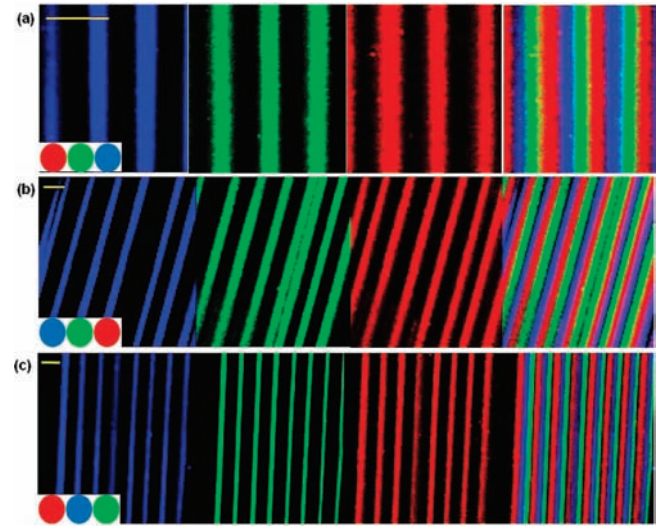

Figure 2. CLSM images showing top views of tricompartmental microfiber scaffolds made by electrohydrodynamic cospinning. The insets indicate the number, spatial configuration, and fluorescence labeling of the streams. Blue, green, and red micrographs representing fluorescence from MEHPPV, PTDPV, and ADS306PT dyes, respectively, are shown independently from left to right, followed by the overlay of the three individual fluorescence images. All scale bars represent 20 μm.

10.1021/ja900354b CCC: $40.75

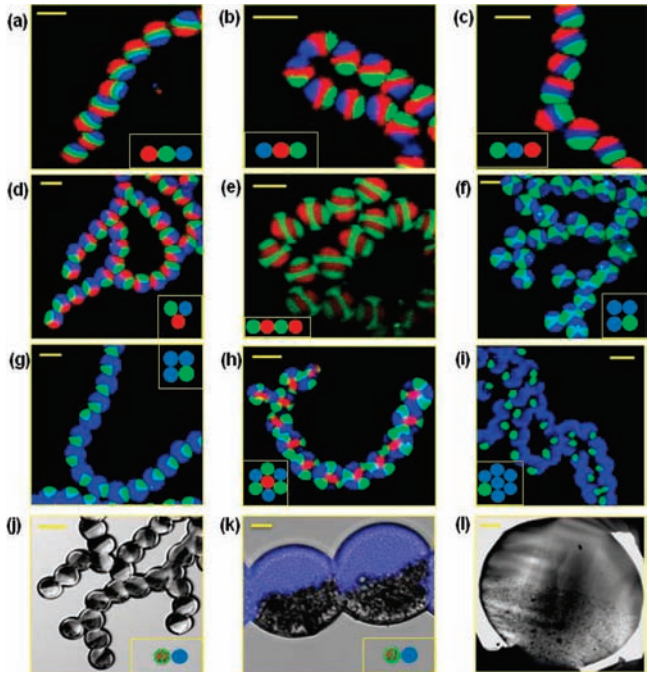

Figure 3. Cross-sectional CLSM images of multicompartmental microfibers with up to seven distinct compartments. Insets indicate the number, spatial configuration, and nature of the outlet streams used during electrohydrodynamic cojetting. (a−c) Tricompartmental microfiber isomers: (a) {sRGB}; (b) {sBRG}; (c) {sRBG}. (d) Multicompartmental microfiber scaffold with a pie-shaped anisotropy, {pRBG}. (e) Tetracompartmental microfiber scaffold showing alternating red and green compartments. (f) Tetracompartmental microfiber scaffold with blue and green compartments. (g) Tetracompartmental microfiber scaffold with one out of four compartments of each fiber labeled with PTDPV, yielding a green "quarter" compartment and a 3-fold larger blue compartment. (h) Heptacompartmental microfiber scaffold resembling a flower. (i) Heptacompartmental fibers with one green compartment that is 6-fold smaller than the other. (j) Differential interference contrast (DIC) micrographs of bicompartmental fibers with magnetite nanocrystals loaded in one compartment only. (k) High-resolution overlay of DIC and CLSM images. (l) Corresponding TEM micrograph. Scale bars represent 20 μm for (a−j), 5 μm for (k), and 2 μm for (l).

Ⓦ A movie showing the Z-stack analysis of the pie-shaped microfiber in (d) is available.

hypothesized that changing the macroscopic arrangement of the outlet streams would result in different fiber isomers. For this purpose, a set of three nozzles was employed for electrohydrodynamic cospinning, where the sequence of the incoming jetting solutions as well as their relative arrangement could be controlled. Great care was taken to ensure that the electrohydrodynamic cojetting conditions were otherwise unaltered. Figure 2a−c shows tricompartmental PLGA fibers formed by placing the three outlet streams of the nozzle in sequence. Placing the green, red, or blue jetting solution into the center space resulted in the {sRGB}, {sBRG} or {sRBG} isomer, respectively. The internal architectures of the tricompartmental microfiber scaffolds were further confirmed by cross-sectional analysis (Figure 3a−d). In contrast to the striped isomers, a triangular arrangement of the outlet flows resulted in the very distinctive {pRGB}-type fiber architecture (Figure 3d). Z-stack analysis of the {pRGB} isomer unambiguously confirmed its unique microstructure (see Figure S5 in the SI and the movie showing the Z-stack analysis of the {pRGB} fiber). We conclude on the basis of these experiments that the electrohydrodynamic cojetting process is well-suited to control not only the exact topology of the deposited fiber scaffolds but also the compartment architecture and presentation.

Next, we elucidated the feasibility of using the electrohydrodynamic cospinning process with four to seven outlet streams to create scaffolds with a larger number of compartments. When the jetting solutions were arranged in an alternating sequence, scaffolds consisting of striped microfibers with four distinguishable compartments in series were prepared (Figure 3e). However, when a square arrangement of the outlet flows was used, the compartments of the microfibers were arranged as rosettes of alternating compartments (Figure 3f). Similarly, more complicated rosettes consisting of seven compartments were prepared (Figure 3h). An exciting aspect of the ability to precisely control the internal fiber architectures is that not only compartment arrangement but also the relative size of compartments can be controlled. Figure 3g,i shows bicompartmental microfiber scaffolds with asymmetric compartment sizes. In these examples, one compartment was 3- or 6-fold larger than the other compartment. With electrohydrodynamic cojetting, the synthesis of these microfibers can be achieved simply by charging an appropriate number of outlet flows with identical jetting solutions, and the relative compartment sizes can be controlled with high accuracy. Finally, we explored the possibility of creating organic/inorganic hybrid materials in which one compartment consists of a PLGA/magnetite nanocomposite while the other contains PLGA only (Figure 3j). The magnetite nanocrystals are clearly confined in one of the two compartments. This is further confirmed by the high-magnification image (Figure 3k) and TEM analysis (Figure 3l), which show the sharp interface formed between the two compartments.

Multicompartmental microfiber scaffolds point toward a new chemistry-based pathway of overcoming key challenges in a number of biotechnological applications, such as spatial control over cell-adhesive properties of three-dimensional scaffolds. In terms of scaffold design, a series of new design parameters have been introduced that have the potential to play a vital role in the development of the next generation of scaffold materials for tissue engineering, namely, (i) internal fiber architecture, (ii) spatial configuration of the individual fiber compartments, (iii) long-range alignment of individual compartments within a scaffold, and (iv) precise control of the relative size of individual compartments. Ultimately, microstructured scaffolds may have important implications not only in fundamental biological studies but also in a series of biotechnological applications, including high-throughput screening, coculture of multiple cell types, and regenerative medicine.

Acknowledgment. We thank Chris Edwards (Microscopy and Image Analysis Lab, University of Michigan) for guidance with respect to cryosectioning and Prof. David C. Martin and Dr. Mutsumi Yoshida (University of Michigan) for valuable discussions. J.L. gratefully acknowledges financial support from the American Cancer Society.

Supporting Information Available: Experimental details and individual confocal micrographs showing a sequence of Z-stack images. This material is available free of charge via the Internet at http://pubs.acs.org.

References

(1) Venugopal, J.; Low, S.; Choon, A. T.; Ramakrishna, S. *J. Biomed. Mater. Res.* **2008**, *84B*, 34.
(2) Kwon, I. K.; Kidoaki, S.; Matsuda, T. *Biomaterials* **2005**, *26*, 3929.
(3) Yang, F.; Murugan, R.; Wang, S.; Ramakrishna, S. *Biomaterials* **2005**, *26*, 2603.
(4) Mitragotri, S.; Lahann, J. *Nat. Mater.* **2009**, *8*, 15.
(5) Pham, Q. P.; Sharma, U.; Mikos, A. G. *Biomacromolecules* **2006**, *7*, 2796.
(6) Park, K.; Ju, Y. M.; Son, J. S.; Ahn, K. D.; Han, D. K. *J. Biomater. Sci., Polym. Ed.* **2007**, *18*, 369.
(7) Tian, F.; Hosseinkhani, H.; Hosseinkhani, M.; Khademhosseini, A.; Yokoyama, Y.; Estrada, G. G.; Kobayashi, H. *J. Biomed. Mater. Res.* **2008**, *84A*, 291.
(8) Roh, K. H.; Martin, D. C.; Lahann, J. *Nat. Mater.* **2005**, *4*, 759.
(9) Roh, K. H.; Martin, D. C.; Lahann, J. *J. Am. Chem. Soc.* **2006**, *128*, 6796.
(10) Roh, K. H.; Yoshida, M.; Lahann, J. *Langmuir* **2007**, *23*, 5683.
(11) Yoshida, M.; Roh, K. H.; Lahann, J. *Biomaterials* **2007**, *28*, 2446.
(12) Kazemi, A.; Lahann, J. *Small* **2008**, *4*, 1756.
(13) Gupta, P.; Wilkes, G. L. *Polymer* **2003**, *44*, 6353.

JA900354B